



# A low-power high-gain LNA for the 60GHz band in a 65 nm CMOS technology

Michael Kraemer, Daniela Dragomirescu, Robert Plana

## ► To cite this version:

Michael Kraemer, Daniela Dragomirescu, Robert Plana. A low-power high-gain LNA for the 60GHz band in a 65 nm CMOS technology. Asia Pacific Microwave Conference 2009, Dec 2009, Singapore, Singapore. hal-00449480

**HAL Id: hal-00449480**

**<https://hal.science/hal-00449480>**

Submitted on 21 Jan 2010

**HAL** is a multi-disciplinary open access archive for the deposit and dissemination of scientific research documents, whether they are published or not. The documents may come from teaching and research institutions in France or abroad, or from public or private research centers.

L'archive ouverte pluridisciplinaire **HAL**, est destinée au dépôt et à la diffusion de documents scientifiques de niveau recherche, publiés ou non, émanant des établissements d'enseignement et de recherche français ou étrangers, des laboratoires publics ou privés.

# A low-power high-gain LNA for the 60 GHz band in a 65 nm CMOS technology

Michael Kraemer <sup>#\*1</sup>, Daniela Dragomirescu <sup>#\*2</sup>, Robert Plana <sup>#\*3</sup>

<sup>#</sup>CNRS ; LAAS ; 7 avenue du colonel Roche, F-31077 Toulouse, France

<sup>\*</sup>University of Toulouse ; UPS, INSA, INP, ISAE ; LAAS ; F-31077 Toulouse, France

<sup>1</sup>mkraemer@laas.fr; <sup>2</sup>daniela@laas.fr; <sup>3</sup>plana@laas.fr

**Abstract**—One essential building block for integrated 60 GHz CMOS radio transceivers is the low noise amplifier (LNA). This paper presents a two-stage cascode LNA fabricated in the 65 nm bulk CMOS technology of ST Microelectronics. It occupies 0.4 mm x 0.4 mm die area (pad-limited). For the matching networks, lumped elements are employed exclusively. It can be biased using two different supply voltages: When using 1.5 V, a peak gain of 22.4 dB and an output-referred 1 dB compression point of -3.4 dBm is measured while drawing 11.2 mA supply current. The simulated noise figure is 4.5 dB. When using a supply voltage of 1.0 V, a peak gain of 18.7 dB and an output-referred 1 dB compression point of -6.5 dBm is measured while drawing 8.5 mA supply current. The simulated noise figure is 5.2 dB.

## I. INTRODUCTION

A major research topic in the domain of microwave engineering today is the design of low-cost transceiver front-ends for the unlicensed frequency band around 60 GHz. While the first CMOS circuits for this purpose were designed in a 130 nm technology [1], the use of lower scale CMOS technologies with higher unity gain frequencies ( $f_T$ ,  $f_{max}$ ) is one way to improve performance. However, the potential advantages are accompanied by drawbacks such as lower breakdown voltages (and thus decreased linearity), more stringent density rules and scaling of the metal back-end.

This paper deals with one of the basic building blocks of such a transceiver, the low noise amplifier (LNA), implemented in a 65 nm CMOS technology.

Employing the Friis equation [2] in the form

$$NF_{tot} = NF_{LNA} + \frac{NF_2 - 1}{G_{LNA}} \quad (1)$$

gives the overall noise figure (NF) of a receiver as a function of the NF of the LNA, the NF of the subsequent circuit elements ( $NF_2$ ) and the gain of the LNA. Note that a high LNA gain is thus essential to achieve good receiver performance, because it allows to screen the usually much higher noise figures of the subsequent stages. Consequently, the two major requirements for the LNA are low noise figure *and* high gain.

Concerning linearity, the last block is the most important one, as an equation similar to (1) points out [2]. Because the subsequent mixer stage is usually limiting the linearity of the receiver, it is not sensible to maximize the LNA's linearity at the expense of higher DC power consumption. Moreover,

strong inband interferers are not to be expected in the 60 GHz band, which loosens the requirements on the intermodulation points of the LNA.

In addition to the above mentioned requirements, very low power consumption and small chip area are very important for battery-driven, low cost applications.

## II. DESIGN OF THE LNA

The LNA presented in this paper employs two single-ended cascode stages as illustrated in Fig. 1. The cascode topology allows for good stability and excellent reverse-isolation, which is especially important in direct-conversion architectures. The algorithm of [3] is followed throughout design.

The first stage is optimized for very low noise. Therefore, the transistors are biased around minimum NF current density at 0.15 mA/ $\mu$ m [4]. The widths of the transistors M1 and M3 are chosen to be  $22 \times 1 \mu$ m in order to yield a real part of the optimum noise impedance  $R_{SOPT}$  that equals 50  $\Omega$  to facilitate matching. All transistors used in the design have a minimum drawn gate length of 60 nm.

The inductor  $L_{m1}$  forms an artificial transmission line together with the parasitics of M1 and M3, and thus increases the  $f_T$  of the cascode. The value of  $L_{m1}$  is 87 pH. A degeneration inductor is added at the source of M1 to allow a simultaneous

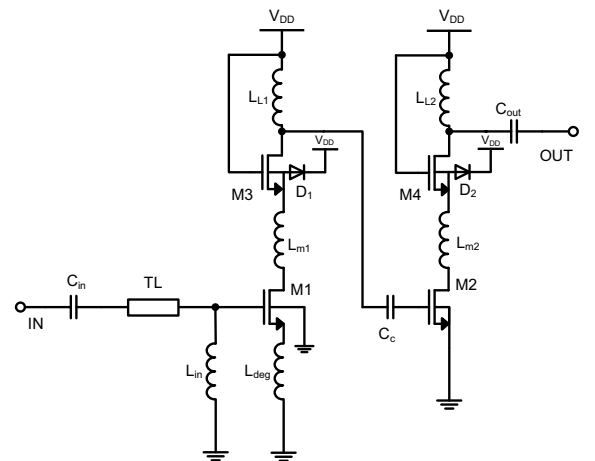


Fig. 1. Simplified schematic of the designed two-stage cascode LNA (parasitic diodes  $D_1$  and  $D_2$  due to deep n-wells surrounding M3 and M4)

noise and power match of the LNA input. Using  $L_{\text{deg}} = 97 \text{ pH}$ , the real part of the input impedance yields around  $50 \Omega$ , without changing  $R_{\text{SOPT}}$ .

The input of M1 has to be matched to the  $50 \Omega$  source impedance in parallel with the  $25 \text{ fF}$  pad capacitance. Because the imaginary part of the optimum noise impedance  $X_{\text{SOPT}}$  is roughly equal to the negative imaginary part of the input of M1, a simultaneous noise and conjugate match is achieved. The matching network consisting of  $C_{\text{in}} = 55 \text{ fF}$ , a  $50 \Omega$  transmission line of length  $25 \mu\text{m}$ , and  $L_{\text{in}} = 139 \text{ pH}$  is designed using the Smith chart for a match around  $60 \text{ GHz}$ .

The second stage is optimized for high gain. Therefore, the transistors are biased at the maximum  $f_T$  current density [5] around  $0.3 \text{ mA}/\mu\text{m}$ . The transistors M2 and M4 have a width of  $26 \times 1 \mu\text{m}$  and thus are slightly larger than M1 and M3 for improved linearity of this second stage. The middle inductor for the second stage was chosen to be  $L_{\text{m2}} = 73 \text{ pH}$ .

The input and output of the second stage are power matched to the preceding stage and the load impedance ( $50 \Omega$  in parallel to the pad capacitance). The values for the input matching network are  $L_{\text{L1}} = 125 \text{ pH}$  and  $C_C = 210 \text{ fF}$ , the values for the output matching network are  $L_{\text{L2}} = 139 \text{ pH}$  and  $C_{\text{out}} = 38 \text{ fF}$ . The maximum allowable supply voltage used for the cascode stages depends on the transistors employed. Generally, a higher  $V_{\text{DD}}$  yields higher performance at the expense of increased power consumption. While the presented circuit was designed for a  $V_{\text{DD}}$  of  $1.5 \text{ V}$ , a lower supply voltage (an example throughout this paper is  $1 \text{ V}$ ) can be employed to reduce power consumption.

#### A. Transistors

The employed  $65 \text{ nm}$  technology provides low power (LP) and general purpose (GP) transistors. The LP transistors offer higher gate oxide thickness and thus reduced leakage currents and an increased breakdown voltage ( $1.2 \text{ V}$  instead of  $1.0 \text{ V}$ ). While in digital designs leakage is directly linked to the static power consumption, in millimeter-wave circuits the transistors are biased at high current densities, compared to which the leakage currents are negligible.

Furthermore, as shown in [5], the LP transistors exhibit an  $f_T$  way below the one of GP transistors (e.g.  $135 \text{ GHz}$  in lieu of  $180 \text{ GHz}$  for  $65 \text{ nm}$  CMOS as presented in [5]). This shows that for a transistor biased at a given power consumption, GP devices exhibit superior performance, mandating their use for low power circuit design.

One consequence of the use of GP transistors is the lower breakdown voltage of  $1 \text{ V}$ . A remedy used during LNA design is to embed the cascode transistors into a deep n-well: In doing so, they are isolated from the grounded substrate and drain and gate voltages in excess of  $1 \text{ V}$  become feasible.

To simulate the behavior of the GP transistors, a BSIM4 model is employed. While the intrinsic performance is well represented by this model, the custom layout is not taken into account. However, the extrinsic performance of the transistors is highly layout-dependent [6]. To obtain an extrinsic model that takes into account the optimized multi-finger layout used,

first, the gate resistance is calculated according to equation (1) of [3]. Secondly, a parasitic extraction is performed. The extrinsic model obtained this way is used during all phases of the LNA design.

#### B. Passive Devices

The passives used during LNA design include capacitors and inductors employed for matching and decoupling. The capacitors used are metal-on-metal (MOM) finger capacitors, because MIM capacitors have too low a quality factor at millimeterwaves.

As inductive matching elements, spiral inductors are used rather than distributed elements. This is possible even at  $60 \text{ GHz}$  because their size remains small compared to the wavelength for the used values. Moreover, their performance with respect to size, realizable values and quality factor are superior to transmission lines when using CMOS technologies with low resistivity substrates [7], [8].

The design of the spiral inductors is done similar to the approach lined out in [8]. However, the focus lies on minimizing the parasitics rather than maximizing the quality factor, which would limit the LNA's bandwidth.

This minimization of parasitics is done by using only the thick top-most metal layers and minimizing both conductor width and total spiral area over substrate. Electromagnetic simulations using HFSS, Sonnet and ASITIC are employed to do quantitative optimizations. Simulations done using these three programs agree very well with each other. The S-parameters obtained by simulation of the final geometry are used to parametrize a  $(2)-\pi$  model, which is employed in linear and non-linear simulations to predict circuit behavior.

The issue of strong coupling between adjacent inductors is addressed by surrounding them by a grounded metal structure consisting of several metal layers. By this means, the path of the ground return current is also clearly defined and can thus be taken into account during electromagnetic simulations.

#### C. Fabricated Circuit

Following the circuit design outlined above, the layout of the circuit is done. Besides the accurately modeled inductors and the small piece of transmission line at the input of the circuit interconnect lengths were short enough to be neglected.

The presented circuit was fabricated in the  $65 \text{ nm}$  CMOS technology of STMicroelectronics with two thick copper metal layers. Fig. 2 shows a photo of the fabricated circuit. Four bias pads and 2 GSG pads for the  $60 \text{ GHz}$  in- and output surround the LNA core.

### III. RESULTS

Measurements up to  $65 \text{ GHz}$  are performed using an Anritsu ME7808A vector network analyzer. A SOLT calibration moves the reference planes to the probe tips. No de-embedding of the pads is required as their capacitance is taken into account by the circuit's matching network.

The measurement of the circuit performance is done at two different bias points: The first *high gain* bias point at  $V_{\text{DD}} = 1.5 \text{ V}$

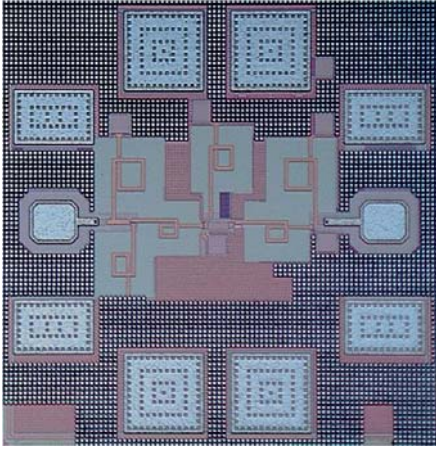


Fig. 2. Photo of the fabricated LNA, circuit dimensions  $400\ \mu\text{m} \times 400\ \mu\text{m}$  including pads.

requires a supply current of 11.2 mA and thus yields a power consumption of 16.8 mW. The second *low power* bias point employs  $V_{\text{DD}}=1.0\ \text{V}$ , drawing 8.5 mA supply current and thus exhibiting a power consumption of 8.5 mW.

The transducer power gain  $G_T$  at these bias points is shown in Fig. 3(a) and 3(b), respectively. Peak gain values of 22.4 dB and 18.7 dB, both at 56 GHz, are achieved, showing good agreement with simulation results.

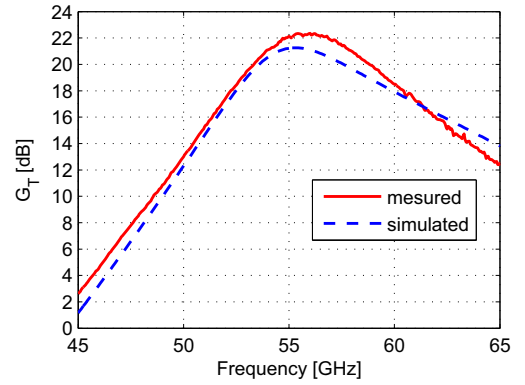
The input and output matching of the LNA at the *high gain* bias point is illustrated in Fig. 4 (for the low power bias point the curves are very similar). A Return loss (RL) inferior to -20 dB is measured around 56 GHz. Furthermore, on the basis of the S-parameter measurements, unconditional stability of the LNA is verified.

In order to quantify the linearity of the LNA, its output power ( $P_{\text{out}}$ ) is measured versus the input power ( $P_{\text{in}}$ ) thus obtaining the -1 dB compression point ( $P_{-1\text{dB}}$ ). In Fig. 5 this curve is plotted together with the uncalibrated gain at the *high gain* bias point. A  $P_{-1\text{dB}}$  of -3.4 dBm is measured, which is sufficient according to the system considerations of section I. For the *low power* bias point,  $P_{-1\text{dB}}$  equals -6.5 dBm (curve not shown). The presented results stem from one single die. Measurements of several other dies of the same wafer confirm the obtained results very closely.

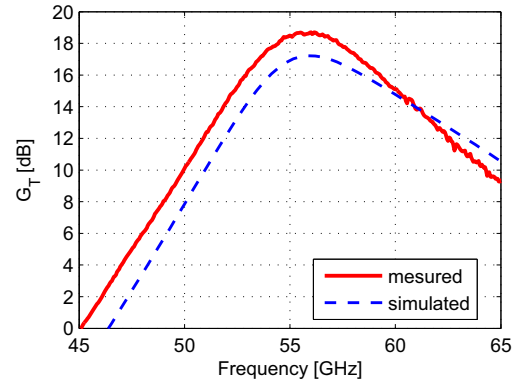
The NF of the LNA has not yet been measured due to lack of measurement capabilities at 60 GHz. The NF simulation results are shown in Fig. 6 for both bias points. Measurement results are expected to be very close due to the use of BSIM4 models and the fact that all parasitics are taken into account during simulation.

#### IV. COMPARISON TO THE STATE OF THE ART

Table I presents a performance overview comparing 60 GHz CMOS LNAs found in literature to the work presented in this paper. General observations are that the noise figure decreases with scaling of technology, and that circuits using lumped elements exhibit smaller size and better over-all performance. The LNA presented in this paper yields low power



(a) supply voltage of 1.5 V



(b) supply voltage of 1.0 V

Fig. 3. Small signal transducer power gain  $G_T$  of the LNA, measurement results versus Cadence SPECTRE simulation

consumption and the best compromise for all LNAs using a cascode topology, showing the interest of using a 65 nm CMOS technology for LNA design. The work presented in [7] shows the interest of using small transistor widths and a more simple common source topology, if the high reverse isolation of a cascode is not necessary.

#### V. CONCLUSION

The high-gain low-power LNA presented in this paper exhibits state-of-the-art performance, yielding the ideal compromise for the input stage of a low-cost low-power 60 GHz receiver. First pass design success was achieved by extracting transistor parasitics and using electromagnetic simulations to model the employed inductors.

Key points in circuit design are the use of inductors, the embedding of the cascode transistor in a deep n-well to allow higher supply voltages, and the use of a 65 nm CMOS technology for low power-consumption and low noise.

To minimize coupling effects, a differential version of this LNA should be implemented if power consumption is less of an issue.

#### ACKNOWLEDGEMENT

Thanks go to Prof. Sorin Voinigescu of University of Toronto and his students for valuable hints on mm-wave circuit design and Alexandre Rumeau for measurement support.

TABLE I  
PERFORMANCE COMPARISON TO LNAs FOUND IN LITERATURE

Ref.	Techn. [nm]	Freq. [GHz]	max. $G_T$ [dB]	$P_{-1dB}$ [dBm]	min. NF [dB]	$V_{DD}$ [V]	Power [mW]	Area [mm <sup>2</sup> ]	Topology	Matching
[1]	130	60	12	+2	8.8	1.5	54	$1.3 \times 1$	3-stage cascode	distributed
[9]	130	56	24.7	+1.8	7.1	2.4	79.2	$0.72 \times 0.67$	3-stage cascode	distributed
[10]	130	53	14	-6	6.1	1.2	10.6	$0.91 \times 0.58$	4-stage common source #	distributed ##
[6]	90	60	12.2	+4	6*	1.0	10.4	$1.27 \times 0.38$	2-stage common source	distributed
[3]	90	58	14.6	-0.5	5.5	1.5	24	$0.4 \times 0.35$	2-stage cascode	lumped
[11]	90	60	16	+1	6	1.8	29	N.A.	2-stage cascode	distributed
[12]	90	64	15.5	+3.8	5.2	1.65	85.8	$1.3 \times 0.4$	2-stage cascode	distributed
[12]	90	64	13.5	N.A.	N.A.	1.26	47.9	$1.3 \times 0.4$	2-stage cascode	distributed
[7]	90	58	15	-4	4.4	1.3	3.9	$0.32 \times 0.44$	3-stage common source	lumped
[13]	65	60	11.5	1.5	5.6	1.2	72	$0.87 \times 0.7$	3-stage common source	distributed
[14]	65**	64	12	-5	8	2.2	36	$0.96 \times 1.05$	2-stage cascode	distributed
this work	65	56	22.4	-3.4	4.5*	1.5	16.8	$0.4 \times 0.4$	2-stage cascode	lumped
this work	65	56	18.7	-6.5	5.2*	1.0	8.5	$0.4 \times 0.4$	2-stage cascode	lumped

\*simulated; \*\*SOI; # current reuse; ## also one inductor used

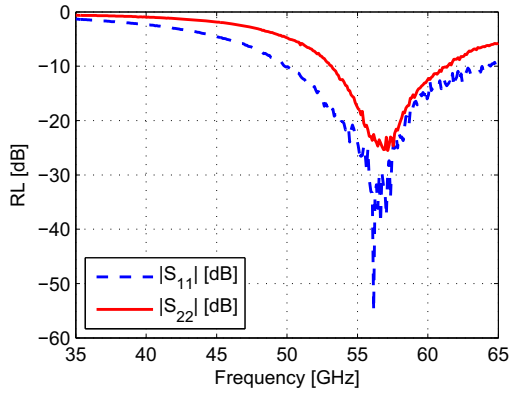


Fig. 4. Return loss (RL) measured at the input and output of the LNA biased at  $V_{DD}=1.5$  V.

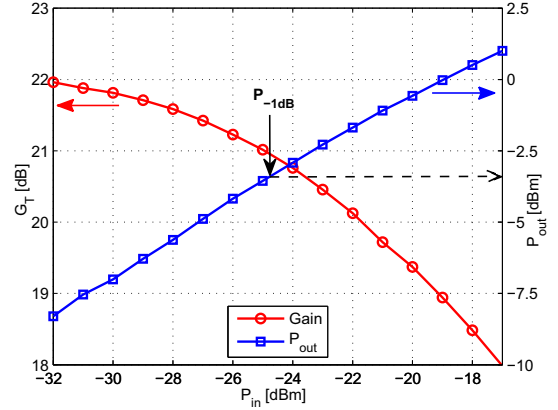


Fig. 5. Plot of measured transducer power gain  $G_T$  and output power  $P_{out}$  versus input power  $P_{in}$  to obtain the -1dB compression point.

## REFERENCES

- [1] C. Doan, S. Emami *et al.*, "Millimeter-wave CMOS design," *IEEE Journal of Solid State Circuits*, vol. 40, no. 1, pp. 144–155, Jan. 2005.
- [2] B. Razavi, *RF microelectronics*. Upper Saddle River, NJ, USA: Prentice-Hall, Inc., 1998.
- [3] T. Yao, M. Gordon *et al.*, "Algorithmic design of CMOS LNAs and PAs for 60-GHz radio," *IEEE Journal of Solid State Circuits*, vol. 42, no. 5, pp. 1044–1057, May 2007.
- [4] S. Voinigescu, T. Dickson *et al.*, "A comparison of Si CMOS, SiGe BiCMOS, and InP HBT technologies for high-speed and millimeter-wave ICs," in *IEEE SiRF*, Sept. 2004, pp. 111–114.
- [5] S. Nicolson, E. Laskin *et al.*, "Design and modeling considerations for fully-integrated silicon w-band transceivers," in *IEEE RFIT*, Dec. 2007, pp. 141–149.
- [6] B. Heydari, M. Bohsali *et al.*, "Low-power mm-wave components up to 104 GHz in 90nm CMOS," in *IEEE ISSCC*, 11–15 Feb. 2007, pp. 200–597.
- [7] E. Cohen, S. Ravid, and D. Ritter, "An ultra low power LNA with 15dB gain and 4.4dB NF in 90nm CMOS process for 60 GHz phase array radio," *IEEE RFIC*, pp. 61–64, April 17 2008.
- [8] T. Dickson, M.-A. LaCroix *et al.*, "30-100-GHz inductors and transformers for millimeter-wave (Bi)CMOS integrated circuits," *IEEE Trans. on MTT*, vol. 53, no. 1, pp. 123–133, Jan. 2005.
- [9] C.-M. Lo, C.-S. Lin, and H. Wang, "A miniature V-band 3-stage cascode LNA in 0.13μm CMOS," *IEEE ISSCC*, pp. 1254–1263, Feb. 2006.
- [10] H.-Y. Yang, Y.-S. Lin *et al.*, "A low-power V-band CMOS low-noise amplifier using current-sharing technique," in *IEEE ISCAS*, May 2008, pp. 964–967.
- [11] S. Pinel, S. Sarkar *et al.*, "A 90nm CMOS 60 GHz radio," in *IEEE ISSCC*, 3–7 Feb. 2008, pp. 130–601.
- [12] S. Pellerano, Y. Palaskas, and K. Soumyanath, "A 64 GHz LNA with 15.5 dB gain and 6.5 dB NF in 90 nm CMOS," *IEEE Journal of Solid State Circuits*, vol. 43, no. 7, pp. 1542–1552, July 2008.
- [13] M. Varonen, M. Karkkainen, and K. Halonen, "Millimeter-wave amplifiers in 65-nm CMOS," in *33rd ESSCIRC*, Sept. 2007, pp. 280–283.
- [14] A. Siligaris, C. Mounet *et al.*, "CMOS SOI technology for WPAN application to 60 GHz LNA," in *IEEE ICICDT*, June 2008, pp. 17–20.

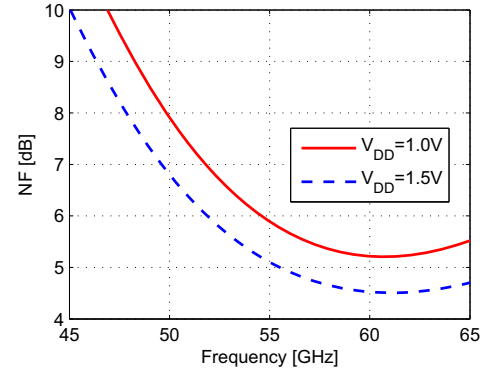


Fig. 6. Simulated noise figure for supply voltages of 1V and 1.5V.